Laminarization of three-dimensional accelerating boundary layers in a curved rectangular-sectioned duct

B. E. Launder and P. A. Loizou
UMIST, Manchester, UK

An experimental study of developing turbulent flow through a rectangular-sectioned bend of decreasing cross-sectional area is reported. Over the first 90° of arc, the duct aspect ratio changes from 1:1 to 3:1 due to the decrease in width of the plane end walls (the width of the curved walls remaining uniform). Two duct Reynolds numbers were selected for study, 8.2×10^4 and 6×10^4, which gave rise to mean values of the acceleration parameter, $\bar{K}$, of 1.5×10^{-6} and 2.1×10^{-6}. Streamwise mean velocity profiles and turbulence intensities were measured at eight stations through the bend with particular emphasis on the near wall velocity profiles on the plane of symmetry of the duct. The present results show a marked thickening of the viscous sublayer and damping of the turbulence intensity due to the acceleration, with the effect being particularly strong on the convex wall where the streamline curvature also acts to inhibit turbulence. At the higher level of acceleration, the boundary layer on this surface reverts essentially to laminar, with the turbulence level being reduced practically to background levels. In contrast, on the concave wall it appears that a greater degree of laminarization occurs at the lower value of acceleration. It is suggested that this unexpected result may be due to differences in the secondary flow pattern between the two test cases.

Keywords: turbulent flow; laminarization; curved ducts; accelerated flow

Introduction

The explorations reported in this paper have been motivated by the problems of flow through stator and rotor passages of gas-turbine blades. While it is usual in computing such flows to regard the strongly accelerated boundary layers on the blade surfaces as two dimensional (2-D), the sharp turning of the flow through the passage in conjunction with the rather small aspect ratios (the ratio of the blade height to the distance between blades) means that in practice three-dimensional (3-D) effects on the boundary-layer development will be significant.

The experiments described below provide data of the flow development in a curved reducing area rectangular duct. The separate effects of streamwise curvature and severe acceleration have been extensively reported in the literature over the past 25 years, and the physical mechanisms responsible are reasonably understood. The behavior of 2-D strongly accelerating flows on plane surfaces have been reported *inter alia* by Launder (1963, 1964), Schraub and Kline (1965), Moretti and Kays (1965), Jones and Launder (1972), and Spalart (1986). The last of these studies reports a computer simulation of sink-flow boundary layers, giving unprecedented detail of the turbulence structure. There is unanimity among these explorations that the dimensionless acceleration parameter

$$K \equiv \frac{\nu}{W_\infty^2} \frac{dW_\infty}{dz} \qquad (1)$$

(z being the stream direction and W_∞ the free stream velocity) provides a good indicator of when the near wall viscous sublayer will grow thicker than in a conventional turbulent boundary layer and, eventually, for sufficiently high values of K, will lead to a reversion of the complete boundary layer to laminar. In fact, Spalart's study indicates that accelerations with sustained levels of K above 2.8×10^{-6} lead to such a laminarization (a result consistent with less precisely identified limits reported in the earlier experimental studies) while perceptible thickening of the viscous sublayer is evident for values of K above 1.0×10^{-6}.

In turbulent boundary layers on curved walls, it is well known that appreciable effects of streamline curvature arise even when the boundary-layer thickness is as small as 1 percent of the wall radius (Bradshaw 1973). When the fluid's angular momentum increases with radius, corresponding to a convex wall, turbulent mixing is inhibited and usually a rapid drop in wall shear stress results. On the concave wall augmented mixing results, often accompanied (or, some would argue, caused) by the formation of streamwise Görtler vortices formed in counterrotating pairs.

From these separate effects of streamline curvature and acceleration one may infer that in a curved, reducing area duct considered in the present work, the boundary layer on the convex wall would revert toward laminar for a smaller value of K than on a flat plate, while that on the concave wall would require a larger value. There is, moreover, the contribution of the secondary flow induced by the duct's curvature, which carries fluid from the outside to the inside of the bend in a rather thin region close to the flat end walls. There will be a corresponding return flow over the core of the duct from the inside to the outside. If, as here, the boundary layers on the inner and outer walls do not join, the secondary flow will produce an impingement of low turbulence intensity fluid on the concave outer wall, continually thinning the boundary layer

Address reprint requests to Dr. Launder at the Department of Mechanical Engineering, UMIST, P.O. Box 88, Manchester M60 1QD, UK.

Received 12 July 1991; accepted 11 November 1991

there. The secondary flow likewise thickens the boundary layer near the mid-plane of the inner wall. It is difficult to foresee what changes in the overall boundary-layer structure might be brought about by the secondary motion; there do not appear to be grounds for supposing that they will be negligible, however. Indeed, we argue later that differences in the secondary flow pattern at the two levels of acceleration are probably responsible for the curiously unexpected differences in the concave-wall boundary layer in the two experiments.

The experimental apparatus, instrumentation, and data collection procedures are briefly described in the next section. A more complete account is provided by Loizou (1989). The results themselves are discussed, following which conclusions are drawn. A companion paper (Launder and Loizou 1992) considers the problem of predicting this complex 3-D flow with a hierarchy of engineering turbulence models and concludes that no level short of second-moment closure within the near wall sublayer will achieve an adequate prediction of the wall friction and heat transfer rates.

Apparatus and instrumentation

A schematic view of the apparatus is shown in Figure 1. Air is drawn into the perspex test section from the laboratory through a 5.6:1 area contraction. The boundary layers on the walls of the square-sectioned inlet duct were tripped at 1.5 hydraulic diameters downstream from the end of the inlet contraction by copper wire, 0.25 mm in diameter, cemented to the walls. The length of the straight inlet section was $5D_H$, the duct terminating in a flange by means of which it was bolted to the correspondingly flanged 180° bend section. In fact, as indicated in Figure 1a, a short region of the bend section was also straight so that, including the relevant flanges, the initial straight section amounted in total to $6D_H$.

Particular care was taken in constructing the variable area curved section to achieve the smallest tolerances and to ensure rigidity and freedom from leaks. Loizou (1989) provides full details but, for illustration, perpendicularity of abutting walls was within $\pm 0.2°$, while duct dimensions and radii of curvature were within 0.38 mm (0.015 inches) of the nominal values given in Figure 1a. Over the first 90° of arc the inner and outer curved walls of the duct are defined by circular arcs of radius R_{out} and R_{in} of 343 mm and 254 mm. Because of the displacement of the centers of curvature, the straight section of the inner wall extends 59.3 mm further than on the outer wall. The offsetting of their centers leads to a 3:1 area contraction by the 90° position (the distance between the flat end walls of the test

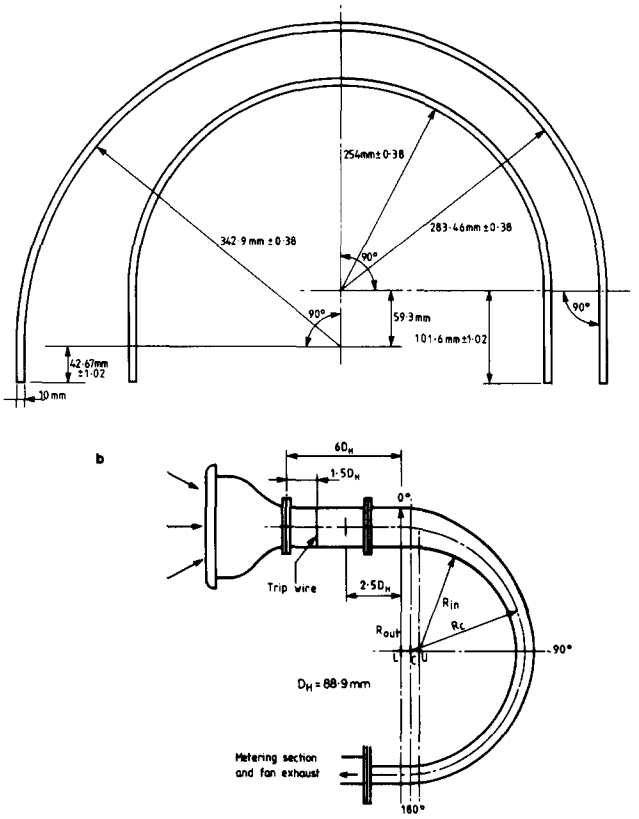

Figure 1 Schematic view of apparatus. (a) Defining dimensions of curved test section; (b) overall view of apparatus

section remaining uniform). Beyond 90° the duct's cross section remains uniform. This is achieved by shifting the center of curvature of the outer wall to coincide with that of the inner wall. No detailed measurements have so far been taken in this second half of the bend. It was included partly to avoid the adverse pressure gradient that would have arisen on the inner wall had the duct become straight at 90°. This choice also facilitated interfacing with an existing outlet tangent, a flow-metering section, and a centrifugal blower (operating in suction mode) employed by Johnson and Launder (1985) in the study of convective heat transfer in a uniform area U-bend.

Access slots were cut in the flat top wall at approximately 13° intervals around the bend to permit radial and vertical

Notation

D_H	Hydraulic diameter of duct at bend entry (equal to length of the sides of the square cross section, 89.3 mm)
D	Local distance between curved walls
r	Radius (centered at C, Figure 1) of point within duct
r^*	$(R_0 - r)/(R_0 - R_i)$, dimensionless radial coordinate
Re	Reynolds number WD/ν
R_c	Radius of midsection of duct (Figure 1)
R_0, R_i	Distance of radial line center C (Figure 1) to outer and inner surfaces of duct
u'	rms turbulent velocity normal to symmetry plane
w'	rms turbulent velocity in streamwise direction
W	Mean velocity in streamwise direction
W_τ	Friction velocity (referred to appropriate wall)
$\bar{W}$	Bulk mean streamwise velocity
x	Coordinate orthogonal to symmetry plane with origin at plane of symmetry
x^*	$(D_H - 2x)/D_H$
y	Coordinate orthogonal to curved walls (with origin at either wall)
y^+	Normalized distance from curved wall $yW\tau/\nu$
z	Streamwise coordinate
ν	Kinematic viscosity

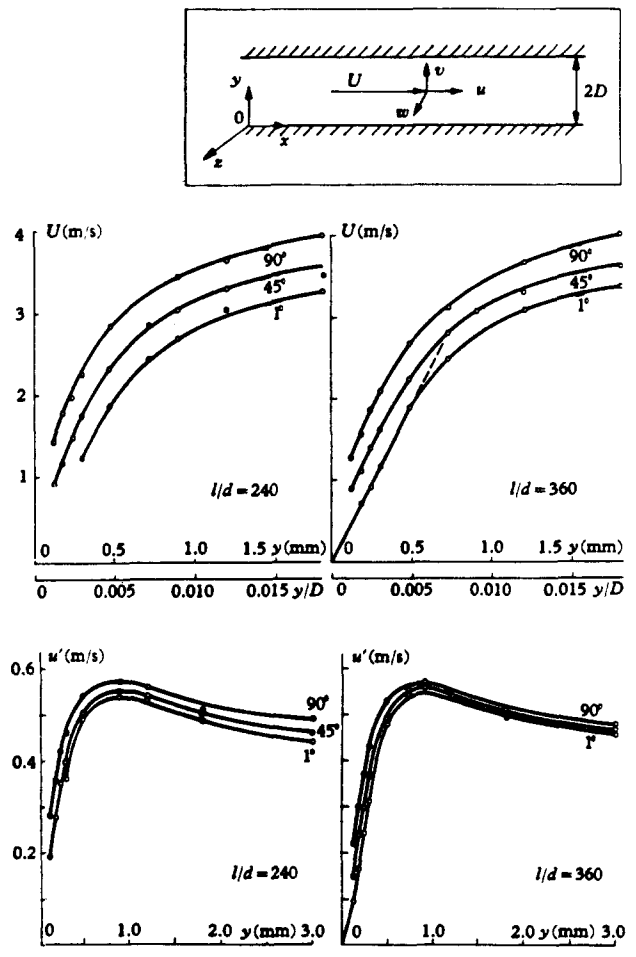

Figure 2 Effect of yaw angle between probe axis and flow direction. (From Van Thinh 1969)

hot-wire traverses; when not in use the slots were sealed by flush-fit perspex plugs. A similar slot in the straight inlet section allowed a full mapping of the velocity profiles at a distance $2.5D_H$ ahead of the curved section. Two different types of hot-wire probes were adopted. A single wire DANTEC 55PO2 probe was used over the inlet cross section and, within the curved duct, for the region very close to the curved walls. Elsewhere in the bend a miniature cross-wire probe (DANTEC 55P63) was employed because of the relatively large radial and tangential mean velocities present.

A two-channel TSI IFA CTA system drove the hot wires. Output was interfaced to a data-acquisition system built at UMIST, which converted the output from the CTA into 12-bit digital records at 250 words per second. Both probes were operated at an overheat temperature of 280 K and calibrated using a TSI Model 1125 Calibrator. Details of the calibration procedure are given by Loizou (1989). We here note simply that the calibration was based on the Siddall and Davies (1972) equation between velocity and bridge voltage, 15 velocity-voltage pairs defining each calibration, with 10^4 discrete voltage readings being stored at each velocity. The single wire was calibrated only at 90°, while the cross-wire probe was calibrated in yaw following established procedures, e.g., Bradshaw (1971).

DANTEC traversing gear was adopted mounted so that, in the direction normal to the plane of symmetry, a resolution of 0.1 mm could be achieved, while in the radial (horizontal) direction the resolution was 0.01 mm. This finer resolution allowed a detailed exploration of the velocity variation very close to the concave and convex walls.

Estimated uncertainties of mean and rms turbulent velocities obtained with the cross-wire probe are taken over from those reported by Iacovides *et al.* (1990) in a uniform area U-bend using the same instrumentation as the present study. These are ± 3 percent and ± 6 percent for mean and fluctuating streamwise components, respectively. Although mean velocities in the direction (x) normal to the symmetry plane were extracted from the data, because their values are much smaller than those of W their experimental uncertainty is too large to justify reporting them here.

In many respects the single-wire data taken within the sublayer on the symmetry plane provide the most interesting results. From a consideration of the many factors likely to affect the results, Loizou (1989) concluded that the greatest uncertainty by far was associated with that induced by the inevitable yaw of the hot-wire probe with respect to the flow direction. Van Thinh (1969) has made an extensive study of this effect. Figure 2, taken from his report, shows the substantially different sublayer mean velocity profiles as the probe axis was changed from being essentially parallel to the wall (1°) to orthogonal to it (90°). However, for angles below 45° with wire length to diameter ratios of 360 (approximately that in the present study), he found that the errors due to finite angles translated simply to an effective displacement of the probe position. Data obtained at finite probe angles could therefore be corrected by applying a lateral displacement in order that the measured velocity profile should extrapolate smoothly to zero velocity at the wall. In the present study a limited exploration of the sensitivity to probe-axis yaw was made at the station upstream of the bend; broadly the same effects reported by Van Thinh were noted. In the present explorations within the bend itself the probe angle varied with position in the duct, the maximum angle being 30°. Accordingly, in all cases where the mean velocity profiles were clearly enough defined in the viscous sublayer to allow an extrapolation to zero velocity to be made, a distance displacement has been applied to all readings to make the zero velocity point corresponding with the wall surface. At a few positions (at 77° and 90° for Re = 82,500 and 90° for Re = 60,000) the sublayer was not adequately resolved and in these cases no correction has been applied. In the cases where a correction has been possible, uncertainties in mean streamwise velocity are estimated at ± 4 percent except for distances from the wall less than about 8 wall units (y^+). Where no correction has been possible, the uncertainty may be as high as 10 percent for the positions closest to the wall; the uncertainty naturally decreases with distance from the wall as the velocity profile becomes flatter. Wall friction has been estimated by the slope of the velocity profile at the wall, an approach that we estimate allows the skin friction coefficient to be obtained with an accuracy of ± 10 percent. Support for this estimate is provided by the fact that upstream of the bend where acceleration and curvature effects are absent, the velocity profile in wall coordinates aligns well with the usual near wall logarithmic profile, as we should expect it to.

Experimental results

Experiments have been undertaken at two Reynolds numbers, based on bulk mean velocity and distance between the curved walls: 82,500 and 60,000. If we define a bulk acceleration parameter, $\bar{K}$, analogous to Equation 1 based on bulk

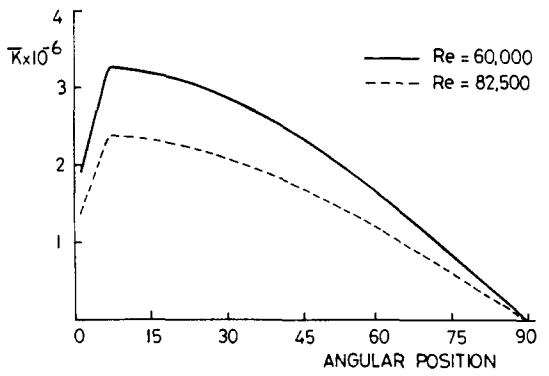

Figure 3 Variation of bulk acceleration parameter $\bar{K}$ around the duct

streamwise velocity at any section

$$\bar{K} \equiv \frac{\nu}{\bar{W}^2}\frac{d\bar{W}}{dz} \tag{2}$$

and evaluate $\bar{W}$ and $d\bar{W}/dz$ from the known flow rate and cross-sectional area, the variation of this parameter for the two Reynolds numbers is as shown in Figure 3.

The mean level of $\bar{K}$ at the higher Reynolds number is about 1.5×10^{-6} and, at the lower, about 2.1×10^{-6}. In the present case $\bar{W}$ is only a few percent less than W_∞ so these values can be directly compared with those cited previously for external boundary layers. In a straight duct such uniform acceleration levels would be sufficient to produce a moderate (for $K = 1.5 \times 10^{-6}$) and a substantial ($\bar{K} = 2.1 \times 10^{-6}$) thickening of the viscous sublayer compared with that indicated by the "universal" near wall velocity distribution. In both cases, however, the flow would remain essentially turbulent.

There is, in fact, in this case a substantial variation in $\bar{K}$ through the duct, with higher values earlier and lower values later. This type of variation is fairly typical of those arising on turbine blades. It might be expected, at the lower Reynolds number, that the initially high levels of $\bar{K}$ would induce a strong reversion of the boundary layer toward laminar, but with a gradual reversion back toward turbulent as the flow develops further around the bend. These anticipatory remarks make no attempt to account for flow curvature, however, or of advective effects on the turbulence structure. Evidently the convex surface of the inner wall should assist the reversion to laminar flow.

The streamwise velocity profile at $2.5D_H$ upstream of the bend for Re = 82,500 is shown in Figure 4 measured along the vertical and horizontal bisectors of the duct. There is satisfactory symmetry in the four quadrants, and we note that, due to the characteristics of the contraction, the maximum velocity reaches its peak value close to the wall. The detailed near wall mean and rms velocity profiles along the horizontal bisector at this station are shown in Figure 5, from which we may note that the turbulence velocity profiles on either side of the duct are also satisfactorily similar. The entry conditions at $\mathrm{Re} = 6 \times 10^{-4}$ are essentially the same, the difference in Reynolds number between the tests being too small for the weak effect that this parameter is known to have on the velocity-profile shape to be detectable.

For the higher Reynolds number (i.e., lower $\bar{K}$), the development of the streamwise mean velocity around the duct over the core region is presented for four stations in Figure 6. (Loizou [1989] shows results for eight stations, but the present selection includes all the notable features). Location $x^* = 1$ corresponds with the symmetry plane while $x^* = 0.75, 0.5$, and 0.25 refer to parallel lines located, respectively, 25, 50, and 75 percent of the distance from the symmetry plane to the end wall. Perhaps the greatest difference from the case of the duct of uniform cross-sectional area (Iacovides *et al.* 1990) is that, throughout the development, the maximum mean velocity is located very much toward the inside of the bend ($r^* = 1.0$). With a uniform cross section (and virtually identical inlet boundary layers to those of the present study) the peak velocity at 90° of arc was displaced to the outside of the bend, and the velocity field in general was considerably more complex (Figure 6e). This is a striking indication that the direct influence of the secondary flow on the axial velocity is much less in the present case, even though, according to our computations (Launder and Loizou 1992), the actual level of secondary flow remains roughly comparable.

At the 0° station, the profile along $x^* = 0.25$ shows interesting undulations that appear to be associated with turbulence-driven secondary flows that have developed in the corners in the straight section. The general inviscid shift of fluid toward the inside of the bend at entry displaces these secondary eddies away from the corner along the top wall. Their effects are soon swamped by the much stronger bend-induced vortex, however.

Profiles of the rms turbulent velocity fluctuations for all stations are shown in Figure 7. The oscillatory mean velocity

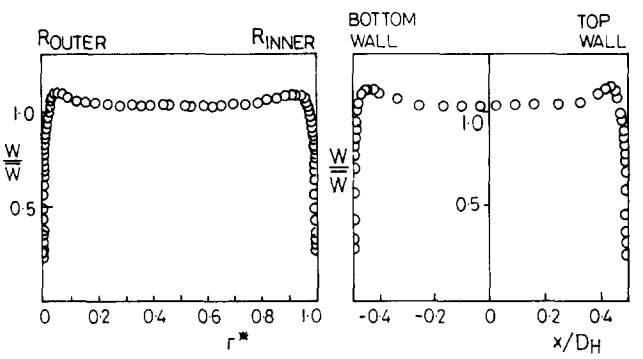

Figure 4 Streamwise mean velocity profiles $2.5D_H$ upstream of bend

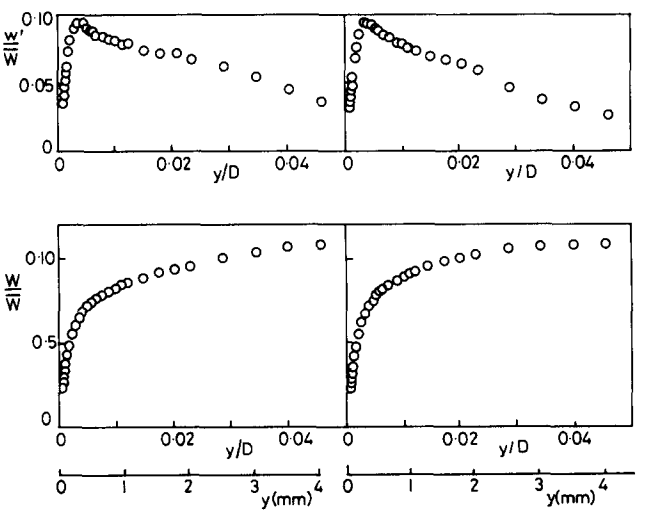

Figure 5 Near wall boundary-layer profiles at $2.4D_H$ upstream of bend; upper, rms velocities; lower, mean velocities; left, outer wall; right, inner wall. $\bar{K} = 1.5 \times 10^{-6}$

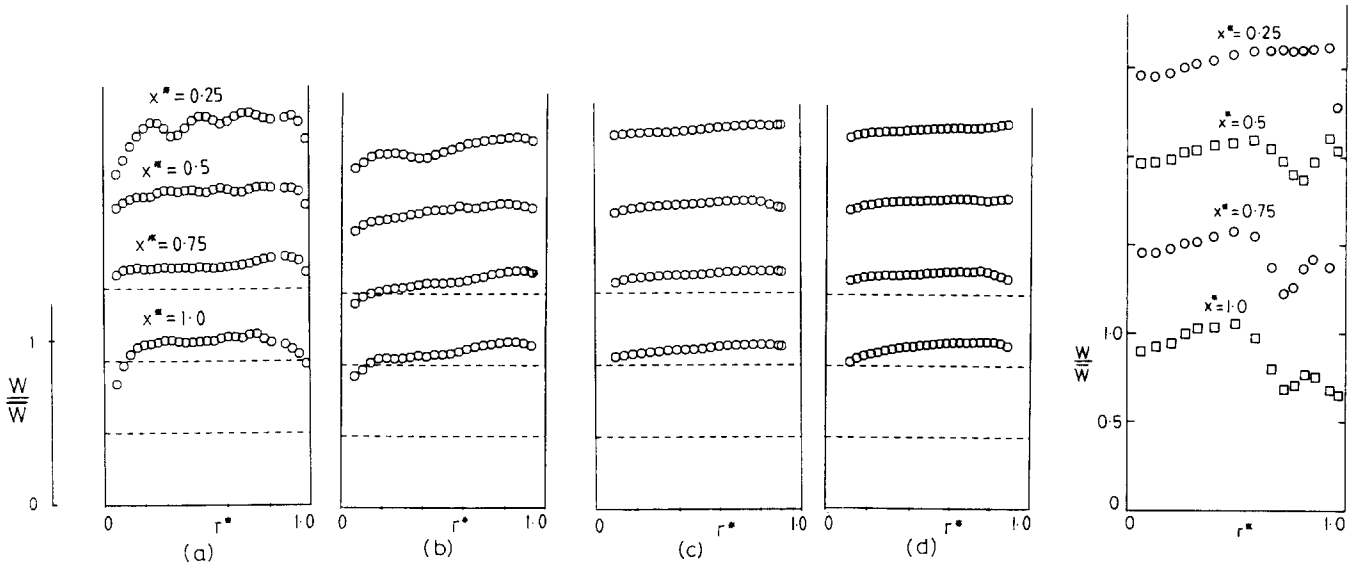

Figure 6 Development of core-region streamwise velocity. Re = 6.0×10^4; $K = 1.5 \times 10^{-6}$. (a) 0°; (b) 26°; (c) 62.5°; (d) 90°; (e) velocity profiles in square duct at 90°. (From Iacovides *et al.* 1990)

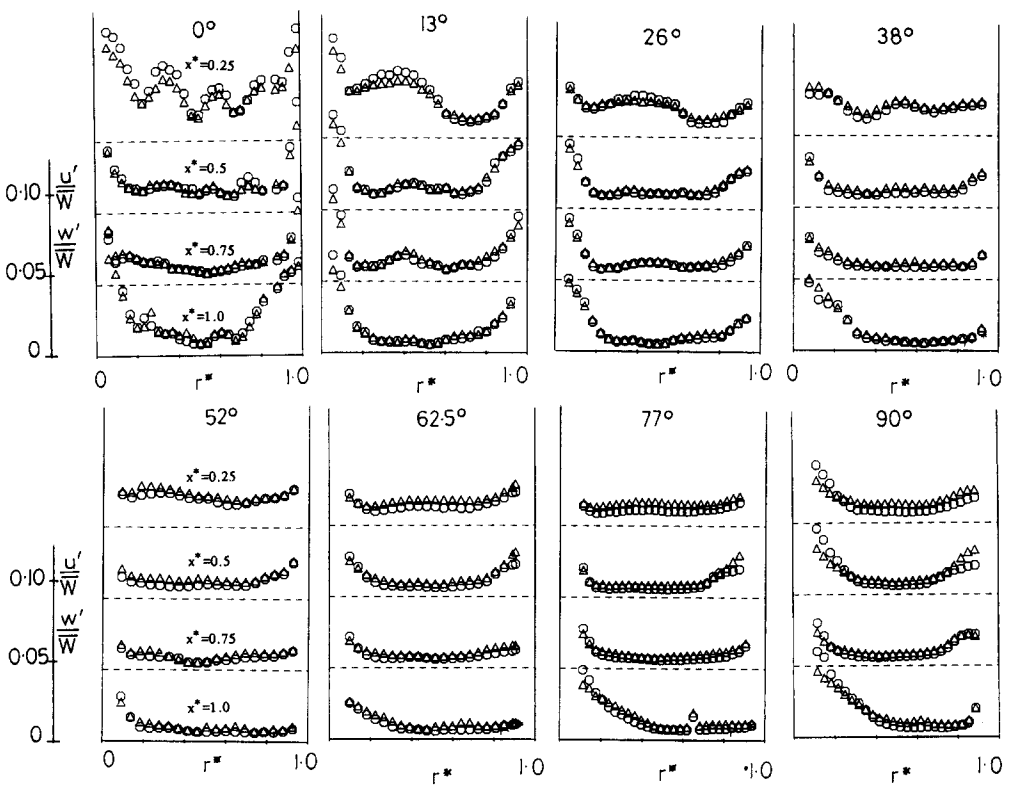

Figure 7 Development of core-region streamwise rms velocity. Re = 6.0×10^4, $K = 1.5 \times 10^{-6}$. ○, $w'/\bar{W}$; △, $u'/\bar{W}$

noted along $x^* = 0.25$ is mirrored by the turbulence intensities: minima in the mean velocity correspond with maxima in turbulence activity, which helps to confirm that the irregularities are associated with a secondary motion. As with the mean velocity, the oscillations quickly disappear. As the flow develops through the contraction the dimensionless turbulence levels fall, being below 1 percent over much of the core by 52°; then, toward the end of the contraction, as K levels diminish, turbulence levels build up again as the boundary layers grow. We note in particular that at 90° the turbulence levels are considerably higher near the concave than the convex surface. Moreover, near the concave wall the streamwise rms fluctuations, w', are clearly higher than those of u' (parallel to the wall but orthogonal to the bulk flow) while near the convex wall, the two fluctuation levels are equal or u' is the larger. These differences in the turbulence field near the two walls broadly accord with the known effects of wall curvature in 2-D boundary layers (Bradshaw 1973).

Far greater detail of the boundary-layer development is provided by the single-wire turbulence intensity measurements

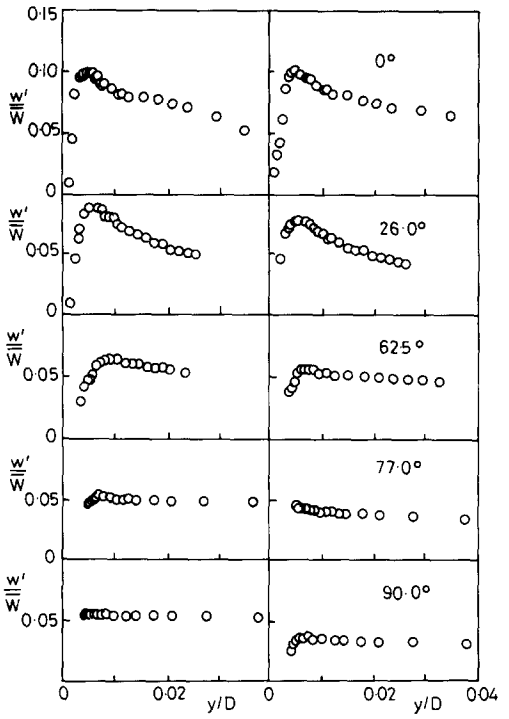

Figure 8 Near wall streamwise turbulence intensity on symmetry plane of duct; $\bar{K} = 1.5 \times 10^{-6}$. Left, concave wall; right, convex wall

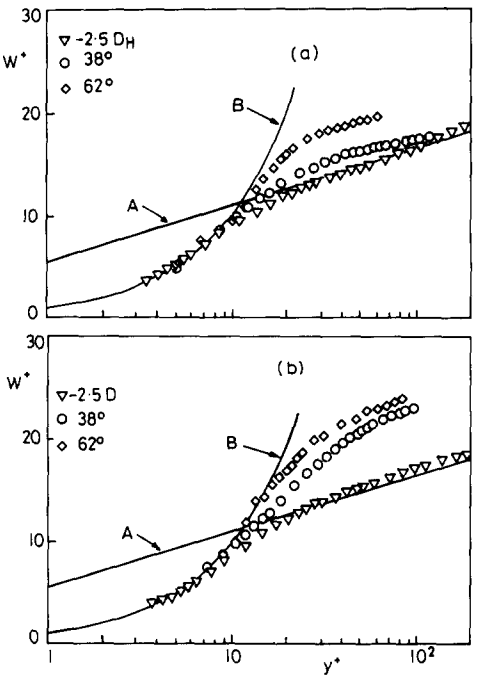

Figure 9 Streamwise velocity profiles on symmetry plane in "universal" coordinates $\bar{K} = 1.5 \times 10^{-6}$. (a) Concave surface; (b) convex surface

on the center plane. The measurements presented in Figure 8 extend to a distance from the wall of only 3–4 percent of the duct width so they are confined within a region not covered by the core-flow measurements. In the plots in Figure 8, the left column relates to the concave wall and the right to the convex. As one proceeds around the bend there is a continual gentle diminution in the level of turbulent velocity fluctuations, the decrease being somewhat more rapid on the convex wall. At 0° the peak turbulence intensity is 0.1 on both walls, while by 77° it is 0.055 and 0.04 on the concave and convex surfaces, respectively. At the 90° station, there is an increase in $w'/\bar{W}$ to 0.06 on the concave surface, while the peak on the convex wall has diminished further to 0.03.

Selected near wall mean velocity profiles are presented in Figure 9 in log-law coordinates. One notes that, as expected, the strong acceleration leads to an overshoot of the velocity profiles above the log law, with the overshoot being more pronounced on the convex surface. Beyond 62° no estimates of wall friction could be obtained, and it is thus not possible to show the further development of the boundary layer on these axes. From the fact that the peak level of w' continues to diminish up to the 77° station and, thereafter, only on the concave wall does it exhibit a slight increase, it seems likely that the mean velocity overshoot would have grown up to the 90° station on the convex surface and that on the concave wall there would have been only a modest reversion toward a normal turbulent boundary layer by the end of the acceleration.

So far as the core region is concerned, there are only minor differences to be discerned between the behavior at the higher acceleration level (average level of $\bar{K} = 2.1 \times 10^{-6}$) and the case considered above. Figure 10 shows the profiles at 0° and 90°; we notice that the turbulence intensities at the latter station are higher and the boundary layer is thicker on the concave than the convex surface. Note, too, that the boundary layer on the convex surface exhibits considerable variation with x^*, being particularly thick and turbulent at $x^* = 0.5$. This

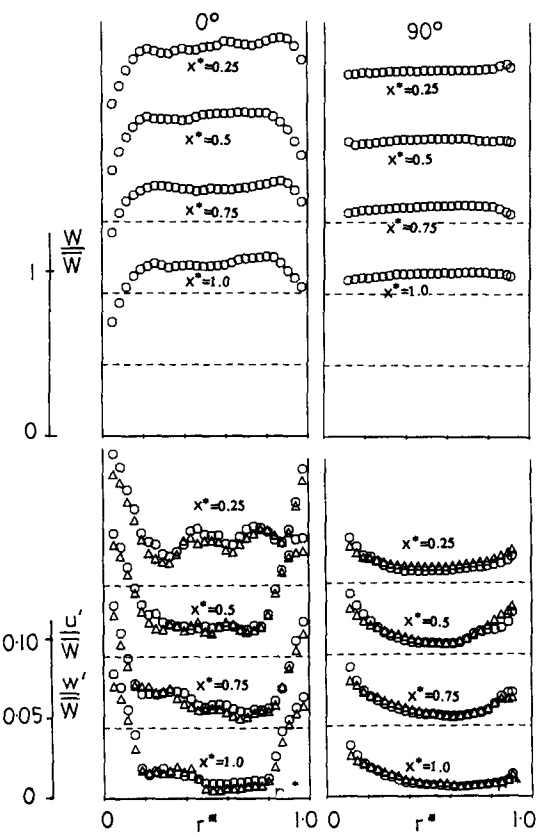

Figure 10 Core region velocity profiles, $\bar{K} = 2.1 \times 10^{-6}$. Upper figures, mean streamwise velocity; lower figures, streamwise turbulence intensity. ○, $w'/\bar{W}$; △, $u'/\bar{W}$

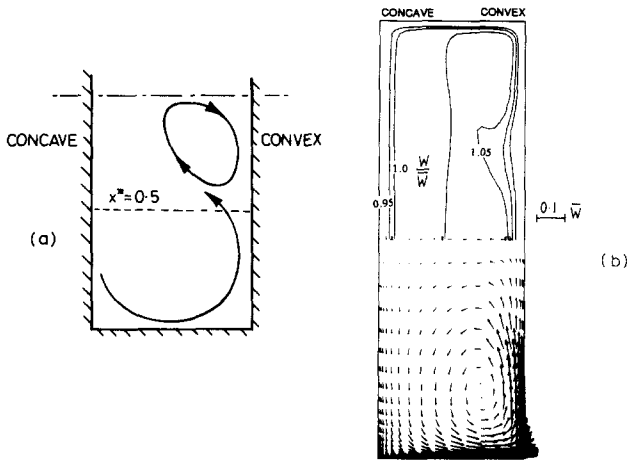

Figure 11 Secondary flow pattern at 90°; $\bar{K} = 2.1 \times 10^{-6}$. (a) Conjectured pattern producing a strong thickening of convex-wall boundary layer at $x^* = 0.5$; (b) computed secondary flow and axial velocity contours (From Launder and Loizou 1992)

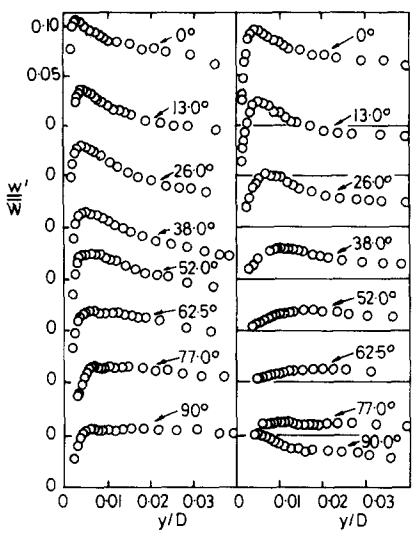

Figure 12 Near wall streamwise turbulence intensity on symmetry plane of duct; $\bar{K} = 2.1 \times 10^{-6}$. Left, concave surface; right, convex surface

variation suggests a separated secondary flow near the convex wall like that shown in Figure 11a, a type of vortex breakdown that does indeed occur in the case of the duct of uniform cross-sectional area (Iacovides *et al.* 1990). The computations of the present flow (Launder and Loizou 1992) do not, in fact, show a vortex breakdown, but they do predict a marked thickening of the convex wall boundary layer in the region of $x^* = 0.5$ (Figure 11b).

The centerline turbulence intensity levels at this higher acceleration level are shown in Figure 12. There is, in this case, a far more rapid collapse of the turbulence on the convex surface, with peak levels being reduced to around 1 percent by the 62° station. Only at the 90° position is there a partial reassertion of turbulence. Paradoxically, on the concave surface beyond the 38° station, the decrease in turbulence intensity with progress around the duct is less than for the lower value of $\bar{K}$. This is such a starting result that one's first reaction must be to question it. The pattern is consistently reproduced at 52°, 62°, and 77°, however. Moreover, the great difference in the boundary-layer structure on the two walls is manifestly evident from the mean velocity profile in linear coordinates, shown in Figure 13 as well as in the log-law plots of Figure 14.

The differences between the behavior at the two Reynolds numbers must almost certainly arise from differences in the secondary flow pattern presumably triggered by the complete collapse to laminar flow on the convex wall and the resultant greater susceptibility to vortex breakdown. If this vortex

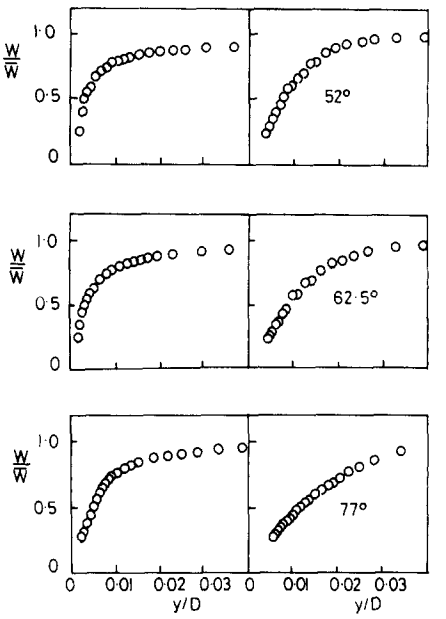

Figure 13 Near wall mean velocity profiles at selected stations; $\bar{K} = 2.1 \times 10^{-6}$. Left, concave surface; right, convex surface

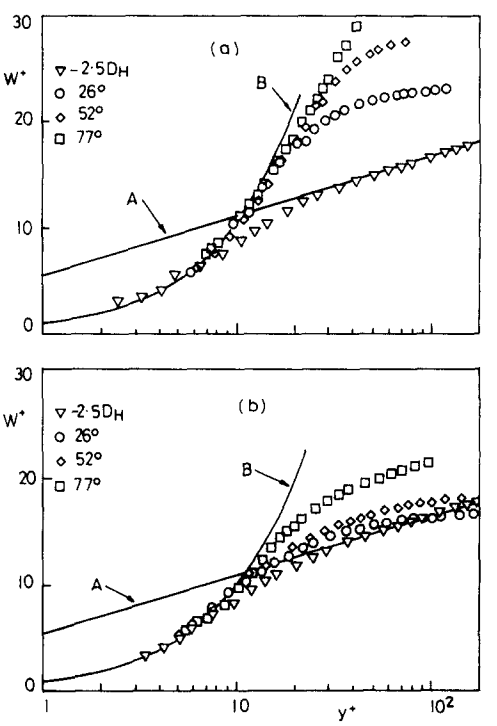

Figure 14 Streamwise velocity profiles in "universal" coordinates $\bar{K} = 2.1 \times 10^{-6}$. (a) Convex surface; (b) concave surface

breakdown were to lead to a significant reduction (or even a reversal) of the secondary flow impinging on the concave wall (as computations for the uniform-area bend suggest can happen, Iacovides *et al.* 1990), this would reduce the thinning of the concave-wall boundary layer, thereby increasing the influence of streamline curvature, which, on the concave wall, increases mixing.

Concluding remarks

The present study of strongly accelerated, 3-D flow around a curved duct has brought out an unforeseen sensitivity to the level of $\bar{K}$ arising from the 3-D character of the flow; this effect is in addition to and significantly modifies the strong sensitivity to $\bar{K}$ found in a 2-D flow.

For a mean level of $\bar{K}$ is 1.5×10^{-6}, the development is broad, as could be anticipated from a knowledge of the separate effects of acceleration and flow curvature on the turbulent boundary layer. That is to say, there is substantial thickening of the near wall sublayer and a diminution of near wall turbulence levels on both convex and concave walls, with a rather greater damping on the convex wall (where curvature acts to suppress turbulence) than on the concave wall (where curvature augments mixing). In fact there is rather less difference between the behavior on the two walls than might be expected given that the boundary-layer thickness midway around the bend is about 4 percent of the wall radius. The relative insensitivity to wall curvature is, we suggest, due to the partially counteracting effect of the flow impingement on the concave surface associated with the bend-induced secondary motion.

For a mean $\bar{K}$ of 2.1×10^{-6} the boundary layer on the convex wall reverts essentially to laminar, but on the concave surface it exhibits a smaller degree of reversion to laminar flow than at the lower $\bar{K}$. This behavior can be explained in terms of a marked modification of the secondary flow arising from the collapse to laminar flow on the convex wall. A laminar flow is more susceptible to vortex breakdown than a turbulent one, and thus a premature secondary separation could halt or even reverse the secondary motion impinging on the concave wall. This in turn would enable the augmented turbulent mixing due to streamline curvature to be more effective. This unforeseen but, with hindsight, explicable development serves to underline, yet again, how difficult it is to anticipate the behavior of 3-D turbulent flows on the basis of observations in 2-D strain fields.

It is hoped that the experimental data here provided will serve as a challenging pair of test cases against which to test and refine engineering turbulence models for complex 3-D flows. Our own experience (Launder and Loizou 1989, 1992) has been that, while the use of a two-equation eddy-viscosity model across the viscous sublayer leads to substantial improvements in predictions over mixing-length and one-equation schemes, the level of agreement even at that level is unsatisfactory. The problem is that the insensitivity of eddy-viscosity models to streamline curvature means that the predicted flow on the convex surface is insufficiently laminarized and, as a result, the conjectured secondary separation from the convex surface does not take place. Thus, it appears that only a model based on second-moment closure (where the representation of momentum transport by way of an eddy-viscosity law is abandoned and one focuses, instead, on equations for the Reynolds stresses themselves) for the whole flow domain, including the near wall sublayer, will provide an adequate physical basis for reproducing the experimental behavior reported above.

Acknowledgments

The research has been jointly funded by the UK SERC and Rolls-Royce under Grant GR/D6567. Extensive technical assistance has been provided by D. Cooper and D. C. Jackson. The keen interest in the research by Dr. N. T. Birch of Rolls-Royce is acknowledged with pleasure. The manuscript has been prepared for publication by J. Buckley. Authors' names appear alphabetically.

References

Bradshaw, P. 1971. *An Introduction to Turbulence and Its Measurements*. Pergamon Press, Elmsford, NY

Bradshaw, P. 1973. Effects of streamline curvature on turbulent flow. *AGARDograph.* **169**

Iacovides. H., Launder, B. E., Loizou, P. A. and Zhao, H. H. 1990. Turbulent boundary-layer development around a square-sectioned U-bend: measurements and computation. *ASME J. Fluid Eng.* **112**, 409

Johnson, R. W. and Launder, B. E. 1985. Local Nusselt number and temperature field in turbulent flow through a heated square-sectioned U-bend. *Int. J. Heat Fluid Flow* **6**, 171

Jones, W. P. and Launder, B. E. 1972. Some properties of sink-flow boundary layers. *J. Fluid Mech.* **56**, 337

Launder, B. E. 1963. The turbulent boundary layer in a strongly negative pressure gradient. MIT Gas Turbine Laboratory, Cambridge, MA, USA, Report 71

Launder, B. E. 1964. Laminarization of the turbulent boundary layer in a severe acceleration. *ASME J. Applied Mech.* **31**, 707

Launder, B. E. and Loizou, P. A. 1992. Assessment of engineering turbulence models for predicting laminarizing flows in curved ducts. Submitted for publication

Loizou, P. A. 1989. Computation and measurement of turbulent flow through idealized turbine blade passages. Ph.D. thesis, Faculty of Technology, University of Manchester, UK

Moretti, P. and Kays, W. M. 1965. Heat transfer to a turbulent boundary layer with varying free-stream velocity and varying surface temperature—an experimental study. *Int. J. Heat Mass Transfer* **8**, 1187

Schraub, F. and Kline, S. J. 1965. A study of the structure of the turbulent boundary layer with and without longitudinal pressure gradients. Rep MD-12 Thermosciences Div., Stanford Univ.

Siddall, R. G. and Davies, T. W. 1972. An improved response equation for hot-wire anemometry. *Int. J. Heat Mass Transfer* **15**, 367

Spalart, P. R. 1986. Numerical study of sink-flow boundary layers. *J. Fluid Mech.* **172**, 307

Van Thinh, N. 1969. On some measurements made by means of a hot-wire in a turbulent flow near a wall. *DISA Inf.* **7**, 13